Experiments in Fluids 23 (1997) 306–316 © Springer-Verlag 1997

Experimental study on the effect of unsteadiness on boundary layer development on a linear turbine cascade

M. T. Schobeiri, K. Pappu

Abstract The results from an experimental investigation of unsteady boundary layer behavior on a linear turbine cascade are presented in this paper. To perform a detailed study on unsteady cascade aerodynamics and heat transfer, a new large-scale, high-subsonic research facility for simulating the periodic unsteady flow has been developed. It is capable of sequentially generating up to four different unsteady inlet flow conditions that lead to four different passing frequencies, wake structures, and freestream turbulence intensities. For a given Reynolds number, two different unsteady wake formations are utilized. Detailed unsteady boundary layer velocity. turbulence intensity, and pressure measurements are performed along the suction and pressure surfaces of one blade. The results display the transition and development of the boundary layer, ensemble-averaged velocity, and turbulence intensity.

List of symbols

c	blade chord
C_p	pressure coefficient $C_p=(p-p_{\text{ref}})/\frac{1}{2}\rho V_{\text{ref}}^2$
d	reference lateral distance from the blade surface, ($=10$ mm)
Re_c	Reynolds number based on the blade chord
Tu	turbulence intensity
U	rotor circumferential velocity, belt translational velocity
V_{ax}	axial velocity
V_u	rotor blade tangential velocity
S_B	blade spacing
S_R	rod spacing
s	streamwise distance from the leading edge of the blade
s_0	streamwise distance from the leading edge to the trailing edge of the blade
t	time
$\langle V\rangle$	ensemble-averaged mean velocity
$\langle v\rangle$	ensemble-averaged fluctuation velocity
y	lateral distance from the surface of the blade
$\langle\gamma\rangle$	ensemble-averaged intermittency factor
λ	turbine stage load coefficient, $\lambda=(V_{u2}+V_{u3})/U$
τ	one wake-passing period
σ	cascade solidity, $\sigma=c/S_B$
φ	flow coefficient $\varphi=V_{ax}/U$
Ω	unsteady flow parameter, $\Omega=\frac{c}{s_R}\frac{U}{V_{ax}}=\frac{\sigma}{\varphi}\frac{S_B}{S_R}$

Received: *23 September 1996/Accepted*: *19 February 1997*

M. T. Schobeiri, K. Pappu
Turbomachinery Performance Laboratory
Texas A&M University, College Station, Texas 77843, USA

Correspondence to: M. T. Schobeiri

1 Introduction

The improvement of efficiency and performance of turbine and compressor stages has been one of the key issues in turbomachinery research and development for several decades. Considerable efforts have been made to develop blade profiles with optimum efficiency for a variety of specific stage-load and flow coefficients (λ, φ) that are encountered in turbine engine design technology. The optimization of blade geometry with regard to the profile loss/efficiency, incidence and deviation range by the industry and research institutions was performed utilizing steady flow cascade experiments. As a rule, the implementation of these profiles into the turbine component was associated with discrepancies in efficiency behavior that were corrected using empirical correlations. These discrepancies are partially attributed to the unsteady nature of the turbomachinery stage flow, which does not exist in steady cascade measurement. The unsteady flow is induced by the alternate change of the absolute and relative frame of references represented by the stator and rotor cascades and viceversa. Earlier experimental research work by Speidel (1957) dealt with the effect of unsteady flow on a single profile. Speidel used a symmetric profile and an oscillating wire to generate the unsteady flow and found a direct correlation between the Strouhal number and the profile loss coefficient. He attributed the increase of the profile loss coefficient to the decrease of the length of laminar boundary layer. Although the research facility by Speidel did not simulate the real periodic unsteady flow situation, the results indicated the significance of the unsteady flow effect on the blade profile loss.

1.1 Modeling the unsteady flow

The significance of the unsteady flow effect on efficiency and performance of compressor and turbine stages was recognized in the early seventies by several researchers. Fundamental studies by Pfeil and Pache (1977), Pfeil and Herbst (1979), Pfeil et al. (1983), and Orth (1993) investigated the effect of unsteady wake flow on the boundary layer transition along flat plates. Pfeil and Pache (1977) simulated the periodic unsteady inlet flow and studied its influence on boundary layer development

under adverse and favorable pressure gradients. They utilized a wake generator with a series of cylindrical rods arranged circumferentially on two parallel rotating disks (squirrel cage type) positioned upstream of the test objects. Using a flat plate and a NACA-65010 airfoil as the test objects for boundary layer investigations, Pfeil and Pache (1977) concluded that the existing calculation methods based on experiments with artificially increased stochastic turbulence of external flow are poorly applicable to their test cases. In continuing the above research work, Pfeil and Herbst (1979), Herbst (1980), and Pfeil et al. (1983) concentrated their efforts on investigating the transition process of unsteady boundary layers. Using a flat plate and varying the pressure gradient, the unsteady inlet flow condition by changing the number, diameter, and frequency of the rods, Pfeil et al. generated wake induced transition, where intermittently laminar and turbulent states of the boundary layer were observed. Their studies showed that the wakes generated by the rods affect the onset and length of transition, particularly if the flow is subjected to a favorable pressure gradient. They established an unsteady boundary layer transition model, which is generally accepted. Priddy and Bayley (1988) and Liu and Rodi (1989, 1991) concentrated their efforts on heat transfer and boundary layer investigations using a similar type of wake generator. Using the flat plate data by Pfeil and Herbst, the turbine data by Dring et al. (1986), and the cascade data by Wittig et al. (1988), Mayle (1991) created a correlation for intermittency distribution.

The above boundary layer research program by Pfeil was continued very recently by Orth (1991, 1993), whose comprehensive research work deals with the boundary layer transition on a flat plate periodically disturbed by wakes. Orth found that a boundary layer flow periodically disturbed by wakes differs in two ways from a boundary layer developing in an undisturbed flow. First, an early onset of transition is observed momentarily as the high turbulence level of the wake disturbs the boundary layer and leads to the formation of turbulent patches. Second, laminar becalmed regions are formed behind the turbulent patches, so that brief periods of laminar flow are still observed beyond the location at which the steady flow boundary layer is fully turbulent.

Schobeiri and Radke (1994b) experimentally investigated the effects of periodic unsteady wake flow and pressure gradient on the boundary layer transition and development along the concave surface of a constant curvature plate. The measurements were carried out under zero and negative pressure gradients using an unsteady flow research facility with a rotating cascade of rods positioned upstream of the curved plate. Boundary layer measurements with hot-wire probes were analyzed using the ensemble-averaging technique. Based on the comprehensive experimental investigations, Schobeiri and Radke concluded that the wake-induced unsteady flow significantly affects the boundary layer transition behavior, which leads to the formation of a primary boundary layer with quasi-steady character and a periodic unsteady secondary boundary layer, generated by the interaction of the wake strip and the wall. The onset of the primary boundary layer and the location of its high turbulence intensity core shifted toward the plate leading edge when subjected to periodic unsteady wakes. As they pointed out, this shift was very likely due to the increased turbulence intensity of the freestream caused by the intense mixing of the incoming wakes. The secondary boundary layer periodically disturbed the laminar boundary layer leading to periodic transition.

Earlier investigations by Eifler (1975) and Trost (1975), utilized a rotating cylinder cascade concept to generate periodic unsteady inlet flow upstream of an annular turbine cascade. While Eifler was primarily interested in the wake development and decay process, Trost's efforts were concentrated on the effect of the wakes on turbine cascade losses. Simoneau et al. (1984) developed a similar research facility to investigate blade heat transfer aspects under unsteady flow conditions. This facility also served to investigate the turbulence structure and wake propagation reported by Morehouse and Simoneau (1986), O'Brien and Capp (1989), and O'Brien et al. (1986). Using a similar research facility, Schultz et al. (1989) and Poensgen and Gallus (1991a, b) investigated three-dimensional wake decay characteristics within compressor cascades. Doorly and Oldfield (1985a, b), Ashworth et al. (1985, 1989), and Dullenkopf et al. (1991) applied the above concept of a rotating cylinder to rectilinear turbine cascades for simulating the unsteady shock wave passing and carried out heat transfer investigations. Concerning the turbine stage, concentrated efforts to understand the effect of unsteady wake flow on the enhancement of turbine blade heat transfer coefficient has resulted in a tremendous amount of related papers (see the exhaustive literature review by Mayle 1991 and Schobeiri and John 1994a). Regarding the compressor flow, efforts have been focused on understanding the effect of unsteady wake flow on performance, particularly on the flow separation, rotating stall, and surge (Schultz et al. 1989; Dong and Cumpsty 1990a, b).

1.2
Unsteady turbine cascade investigations

In spite of the above mentioned efforts, comparatively little attempt has been undertaken to investigate and comprehend the impact of the unsteady wake flow on turbine blade aerodynamics, boundary layer transition, and efficiency. To investigate the effect of unsteady wakes on turbine blade aerodynamics, Trost (1975) used a rotating cylinder cascade installed in front of an annular turbine cascade. Generating different turbulence levels by varying the rotational speed of the rotating cylinder, Trost measured the blade loss coefficients of three different turbine cascade types and compared them with those that were obtained from steady measurement. He found that the steady data cannot be transferred to turbine rotors. This is particularly true for cases where the turbine blade was subjected to a laminar separation. Liu and Rodi (1989) carried out boundary layer and heat transfer measurements on a turbine cascade, which was installed in the squirrel cage type wake generator discussed previously. Due to the restricted accessibility of the hot wire probe, the first 30% of both pressure and suction surfaces could not be reached. As a result, in spite of a major experimental effort, the interesting transition events could not be measured. Following the unsteady investigations by Schobeiri et al. (1995), Schulte and Hodson (1996) applied hot film probes to a low pressure turbine cascade and presented the uncalibrated hot film signals which they interpret as the wall shear stress. Since the time-dependent signals of the uncalibrated surface hot film

probes they used did not quantitatively represent the wall shear stress essential for loss calculation, Schulte and Hodson resorted to pneumatic total pressure measurements and adopted the same conclusions drawn by Schobeiri et al. (1995) a year earlier.

2
Objective of present investigation

The above mentioned studies on turbine cascade aerodynamics have largely concentrated on the measurement of blade surface properties such as the wall shear stress. The few boundary layer measurements are not comprehensive enough to provide any conclusive evidence for the interpretation of the boundary layer transition and separation processes and their direct impact on the profile loss, which is a critical parameter for blade design. The objective of this work is to provide a detailed unsteady boundary layer information essential for evaluating the impact of the unsteady wake flow on the blade efficiency.

It is well known that the boundary layer measurement is the most time consuming aerodynamic measurement. Any attempt to increase the number of parameters to be studied would inevitably result in substantial increase of the measurement time. Considering this fact and the objective formulated above, a new research facility with state-of-the-art instrumentation has been developed to study systematically and efficiently the influence of periodically unsteady and highly turbulent flow on turbine and compressor cascade aerodynamics and heat transfer.

3
Experimental research facility

A large-scale, high-subsonic research facility for simulating the periodic unsteady flow has been developed to study cascade aerodynamics. Since the facility is described thoroughly in a recent paper by Schobeiri et al. (1995), only a brief description of the main components is given below.

The research facility consists of a large centrifugal air supplier, a diffuser, a settling chamber, a nozzle, an unsteady wake generator, and a turbine cascade test section (Fig. 1). An air supplier with a volumetric flow rate of 15 m^3 is capable of generating a maximum mean velocity of 100 m/s at the test section inlet. The settling chamber consists of five screens and one honeycomb flow straightener to control the uniformity of the flow. Downstream of the settling chamber is a nozzle, with an area ratio of 6.75 : 1, that accelerates the flow to the required velocity before it enters the wake generator. The nozzle, with an exit cross section of 1000.0×200.0 mm^2, establishes a smooth transition of the flow from the settling chamber to the wake generator. With this tunnel configuration it was possible to achieve, at the nozzle exit, a constant mean fluctuation velocity over a wide velocity range. For a nozzle exit velocity of 30 m/s, a turbulent intensity of $Tu = 0.75\%$ was measured.

Two-dimensional periodic unsteady inlet flow is simulated by the translational motion of a wake generator (see Fig. 1), with a series of cylindrical rods attached to two parallel operating timing belts driven by an electric motor. To simulate the wake width and spacing that stem from the trailing edge of rotor blades, the diameter (2.0–10.0 mm) and number of rods can be varied. The belt-pulley system is driven by an electric motor and a frequency controller. The wake-passing frequency is monitored by a fiber-optic sensor. The sensor also serves as the triggering mechanism for data transfer and its initialization, which is required for ensemble-averaging.

The special design of the facility and the length of the belts enable a considerable reduction of the measurement time. For the present investigation, two clusters of rods with constant diameter are attached to the belts. The cylindrical rods within each cluster have the same spacing. So, it is possible to measure sequentially the effect of two different spacings at a single boundary layer point. To clearly define the influence domain of each individual cluster with the other one, the clusters are arranged with a certain distance between each other. Using the triggering system mentioned above and a continuous data acquisition, the buffer zones between the data clusters are clearly visible. The data analysis program cuts the buffer zones and evaluates the data pertaining to each cluster. Comprehensive preliminary measurements were carried out to make sure that the data were exactly identical to those, when the entire belt length was attached with rods of constant spacing, which corresponded to each individual cluster spacing.

The cascade test section, located downstream of the wake generator, can include up to 7 blades with a height of 200.0 mm and the chord up to 300.0 mm. The blades are inserted between two vertical plexiglass side walls. One sidewall integrates the boundary layer, inlet, and exit traversing slots. For boundary layer investigations, five NASA turbine blades were implemented whose geometry is described in the NASA Report by Schobeiri et al. (1991). One of the blades was specially manufactured for the measurement of pressure distribution.

A computer controlled traversing system is used to measure the inlet velocities and turbulence intensities, as well as the boundary layers on suction and pressure surfaces. The traversing system is vertically mounted on the plexiglass side wall. It consists of a slider and a lead screw that is connected to a d.c. stepper motor with an encoder and decoder. The optical encoder provides a continuous feedback to the stepper motor for accurate positioning of the probes. The system is capable of traversing in small steps with a minimum of 2.5 μm, which is specifically required for boundary layer investigations where the measurement of the laminar sublayer is of particular interest.

4
Instrumentation, data acquisition, and data reduction

The data acquisition system is controlled by a 486-personal computer that includes a 16 channel, 12-bit analog-digital (A/D) board with 8 channel simultaneous sample and hold. Mean velocities and turbulent fluctuations are obtained by using a commercial 3-channel (TSI), constant temperature hot-wire anemometer system. The system has a signal conditioner with a variable low pass filter and adjustable gain. The three channels of the anenometer are connected to the first three channels of the A/D board from which the data is sampled by the computer. A Prandtl probe, placed upstream of the diffuser, monitors the reference velocity at a fixed location. The pneumatic probes are connected to high precision differential pressure transducers for a 2-channel digital readout. A thermocouple is placed downstream of the test section to constantly monitor the flow temperature. The wake generator speed and the passing frequency signals of the rods

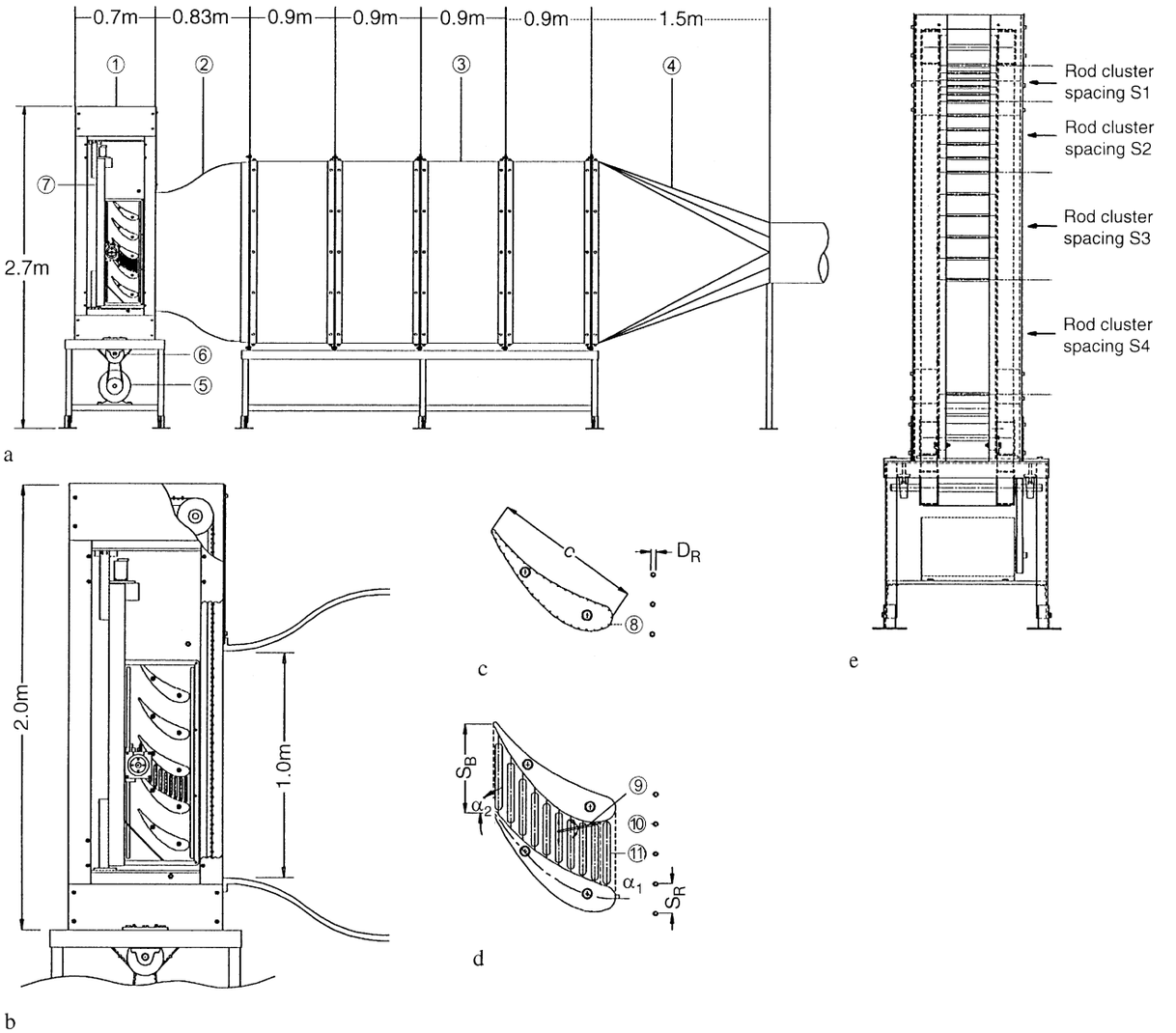

Fig. 1. **a** Test facility: *1* Test section, *2* nozzle, *3* settling chamber, *4* diffuser, *5* motor, *6* belt, *7* traversing system; **b** test section; **c** pressure tap blade: *8* static pressure taps; **d** boundary layer measurement: *9* boundary layer probe, *10* wake generating rods, *11* slots for longitudinal traverse of the probe; **e** cluster configurations for different wake passing frequencies

are transmitted by a fiber-optic trigger sensor. The passage signals of the rods are detected by the sensor using a silver-coated reflective paint on one of the belts. This sensor gives an accurate readout of the speed of the wake generator and the passing frequency of the rods. The signals of the pressure transducers, thermocouple, and trigger sensors are transmitted to the A/D board and are sampled by the computer. Two adjacent blades are used for boundary layer measurement. A third blade was instrumented with 40 static pressure taps, uniformly distributed on the suction and pressure surfaces. The taps were connected to a scanivalve, which sequentially transferred the pressure signals to one of the transducers that was connected to the A/D board.

In order to ensure a high level of accuracy, the calibration method and the facility described in John and Schobeiri (1993) was used for all hot-wire calibrations. The unsteady data were reduced by the ensemble-averaging method (for details, refer to Schobeiri et al. 1995). At each boundary layer position, 16 384 samples were taken at a sampling rate of 20 KHz for each of 50 revolutions of the wake generator. The data were ensemble-averaged with respect to the rotational period of the wake generator. Before final data were taken, the number of samples per revolution and the total number of revolutions were varied to determine the optimum settings for convergence of the ensemble-average.

5
Experimental results and discussion

To investigate the influence of unsteady wake flow on boundary layer development along the suction and pressure surfaces of the turbine blades specified in Table 1, two clusters of cylindrical rods with diameter $D_R = 5$ mm were attached to the

Table 1 Specifications of inlet flow, blade, cascade, and wake generator characteristics

Parameters	Values	Parameters	Values
Axial velocity	$V_{ax}=14$ m/s	Rod diameter	$D_R=5.0$ mm
Blade inlet flow angle	$\alpha_1=0^\circ$	Blade exit metal angle	$\alpha_2=61.8^\circ$
Blade height	$L=200.0$ mm	Blade spacing	$S_B=164.0$ mm
Blade chord	$C=281.8$ mm	Blade *Re*-number	$Re_c=264{,}187$
Cascade solidity	$\sigma=1.76$	Cascade flow coefficient	$\varphi=2.33$
Steady reference point (no rods)	$S_R=\infty$ mm	Ω-parameter steady case	$\Omega=0.0$
Cluster 1 rod spacing	$S_R=160.0$ mm	Ω-parameter for cluster 1	$\Omega=0.755$
Cluster 2 rod spacing	$S_R=80.0$ mm	Ω-parameter for cluster 2	$\Omega=1.51$
No. of rods in cluster 1	$n_R=14$	No. of rods in cluster 2	$n_R=21$

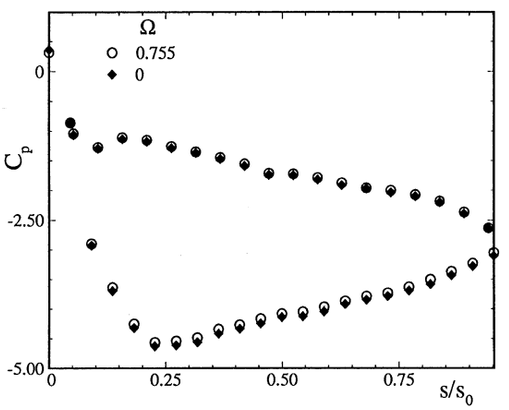

Fig. 2. Pressure distribution at $Re_c=264187$

two belts of the wake generator. This cylinder diameter was chosen to fulfill the similarity criterion that requires the generation of a drag coefficient C_D (see Eifler (1975) for details) that is approximately equal to the C_D of the turbine blade with the chord and spacing given in Table 1. For the flow condition given in Table 1, detailed boundary layer measurements were performed. The diameter of the rods of the two clusters, given in Table 1, is the same and is selected based on the approximate drag coefficient value that pertains to the equivalent profile.

5.1 Surface pressure distribution

The pressure distribution shown in Fig. 2 was taken by a multi-channel scanivalve for a steady ($\Omega=0.0$) and an unsteady case, where rods with one uniform spacing of $S_R=160$ mm, corresponding to $\Omega=0.755$, were attached to the whole length of the belt. The pressure signals inherently signify the time-averaged pressure because of the internal pneumatic damping effect of the connecting pipes to the transducer. The noticeable deviation in pressure distribution between the steady and unsteady cases, especially on the suction surface, is due to the drag of the wake generating rods adding transverse momentum to the flow. No pressure measurements were taken for the current configuration of the belt with two clusters of rods since these measurements would not reflect the true values that would correspond to each individual cluster because of the averaging of pneumatic signals by the scanivalve.

The time-averaged pressure coefficient along the pressure and suction surfaces is plotted in Fig. 2. On the suction surface (lower portion) the flow first accelerates sharply, reaches a minimum pressure coefficient at $s/s_0 \approx 0.25$, and then continuously decelerates at a moderate rate until the trailing edge is reached. On the pressure surface, the flow accelerates, reaches a minimum pressure coefficient at $s/s_0 \approx 0.1$, and experiences a short deceleration and then accelerates almost continuously at a slower rate. This pressure distribution indicates that the flow on both the surfaces, except for a short distance around $s/s_0 \approx 0.1$, is subjected to a negative pressure gradient until $s/s_0 \approx 0.25$ is reached. Beyond this point, the pressure gradient on the pressure surface remains negative, while on the suction surface, positive pressure gradient prevails. This pressure gradient situation has a very significant effect on the boundary layer development, as we will see later in the corresponding section of this paper.

5.2 Ensemble-averaged boundary layer velocity distributions

Boundary layer profiles were taken for one steady and two unsteady inlet flow conditions on the suction surface at 14 streamwise positions and on the pressure surface at 10 streamwise positions. The velocity profiles reflecting the representative boundary layer behavior will be presented.

Periodic unsteady flow was established by the wake generator, which included two clusters of cylindrical rods that were attached to the timing belts running with a translational speed of $U=6.0$ m/s. To account for the unsteadiness caused by the frequency of the individual wake generating clusters and their spacing, the flow velocity, and the cascade parameters, we define an unsteady flow parameter $\Omega=(c/S_R)\ (U/V_{ax})=(\sigma/\varphi)\ S_B/S_R$ that includes the cascade solidity σ, the flow coefficient φ, the blade spacing S_B, and the rod spacing S_R. Many researchers have used Strouhal number as the unsteady flow parameter, which only includes the speed of the wake generator and the inlet velocity. However, the currently defined unsteady flow parameter Ω is an extension of Strouhal number in the sense that it incorporates the rod spacing (S_R) and the blade spacing (S_B) in addition to the inlet velocity and wake generator speed. The individual cluster configurations with the corresponding Ω-parameter are specified in Table 1.

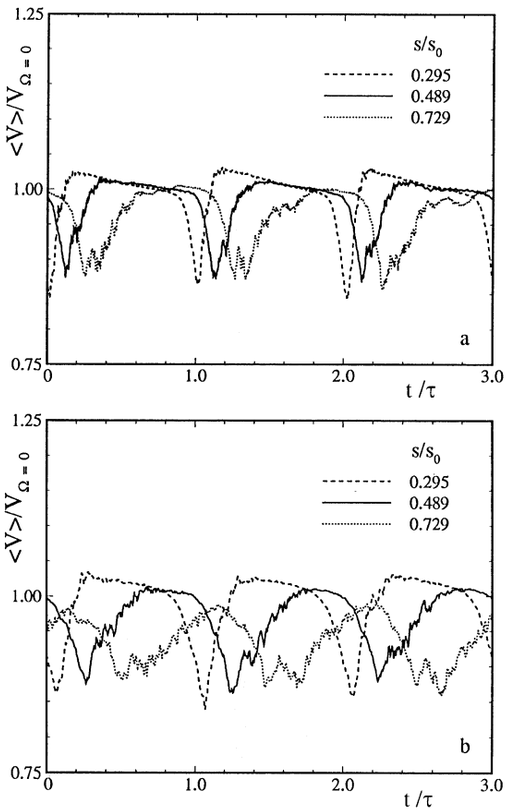

Fig. 3a, b. Ensemble-averaged velocity on pressure surface at $y=2.5$ mm. **a** $\Omega=0.755$; **b** $\Omega=1.51$

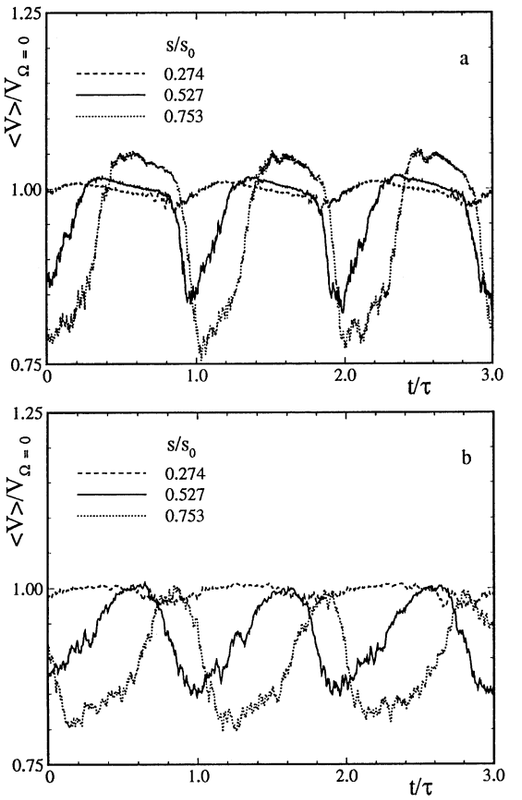

Fig. 4a, b. Ensemble-averaged velocity on suction surface at $y=2.5$ mm. **a** $\Omega=0.755$; **b** $\Omega=1.51$

Experimental investigations were performed for three different unsteady flow parameter values of $\Omega=0.0$, 0.755, 1.51. These values cover the entire reduced frequency range encountered in turbomachinery.

Figure 3 displays the temporal distribution of the ensemble-averaged boundary layer velocity $\langle V\rangle$ for three representative streamwise positions, s/s_0, at $y=2.5$ mm above the pressure surface for those two Ω-values discussed earlier. The choice of the lateral location $y=2.5$ mm is arbitrary and for most streamwise positions it lies inside the boundary layer, except near the leading edge. The velocity is normalized with respect to the velocity of corresponding steady case ($\Omega=0$) at $y=2.5$ mm. For the first half of the profile length on the pressure surface, $s/s_0=0.295$ and 0.489, the velocity distributions in Fig. 3a exhibit an asymmetric behavior indicating the effect of a strong curvature. By convecting further downstream, the diminishing curvature effect, starting at $s/s_0=0.729$, results in an almost symmetric velocity profile. In recent comprehensive theoretical and experimental studies, Schobeiri et al. (1994a) investigated the effect of curvature on the steady and unsteady turbulent wake structure and velocity distribution. In a parallel study, Schobeiri and Radke (1994b) performed detailed boundary layer measurements along a curved plate. In both cases, they observed similar asymmetric behavior of the velocity distributions. They argued that the asymmetric pattern is due to the non-zero pressure gradient in the lateral direction that is characteristic of curved channels. By entering a flow channel, where the lateral pressure gradient approaches a zero value, the asymmetric behavior diminishes. This is clearly shown in the studies by Herbst (1980), Pfeil et al. (1983), Liu and Rodi (1991), and recently by Orth (1991, 1993). They performed unsteady boundary layer transition studies along flat plates inside straight channels, where they measured fully symmetric ensemble-averaged velocity distributions. Further increasing the value of Ω-parameter results in a higher frequency (Fig. 3b) and a slightly lower amplitude of the ensemble-averaged velocity.

Figure 4 shows the temporal distribution of the ensemble-averaged boundary layer velocity $\langle V\rangle$ for three representative streamwise positions, s/s_0, at $y=2.5$ mm above the suction surface for the same two Ω-values discussed above. Starting with $s/s_0=0.274$, the velocity distribution (small-dashed line in Fig. 4a) exhibits an asymmetric behavior with low velocity defect indicating the strong mixing effect due to the high negative pressure gradient on the suction surface. By convecting further downstream, the boundary layer flow on the suction surface undergoes a positive pressure gradient (see also the pressure distribution, Fig. 2) that leads to the recovery of the wake flow at $s/s_0>0.274$. Further increasing the value of the Ω-parameter to 1.51 results in almost symmetric velocity profiles with a higher frequency and a slightly lower amplitude of the ensemble-averaged velocity.

5.3
Periodic unsteady boundary layer, contour plots

Nondimensional velocity distributions on the pressure and suction surfaces with time as the parameter are plotted in semi-logarithmic form in Fig. 5. Here, $\langle V \rangle_{ref}$ refers to the velocity at $y = 10$ mm from the blade surface for the particular time under consideration. The nondimensional time (t/τ) values presented are chosen so that they represent the states starting with the initial state of flow being under the influence of freestream turbulence only to the final state where the flow is totally under the influence of wake. Figure 5a shows the velocity distribution on the pressure surface at $s/s_0 = 0.21$. As can be seen, at time $t/\tau = 0.749$ the wake has not yet arrived and the flow being under the influence of freestream turbulence gives rise to a laminar velocity profile. The time $t/\tau = 0.955$ corresponds to the case where the flow is completely under the influence of wake and correspondingly the velocity profile assumes a turbulent profile. Intermediate times reflect the gradual transition in velocity profiles as the flow is undergoing the influence of the oncoming wake. Figure 5b shows the velocity profiles on the suction surface at $s/s_0 = 0.209$ with t/τ as the parameter. The tendencies discussed with respect to Fig. 5a can also be observed here. More detailed information about the unsteady boundary layer development can be obtained from temporal-spatial domain contour plots of turbulence intensity, which is discussed in the next paragraph.

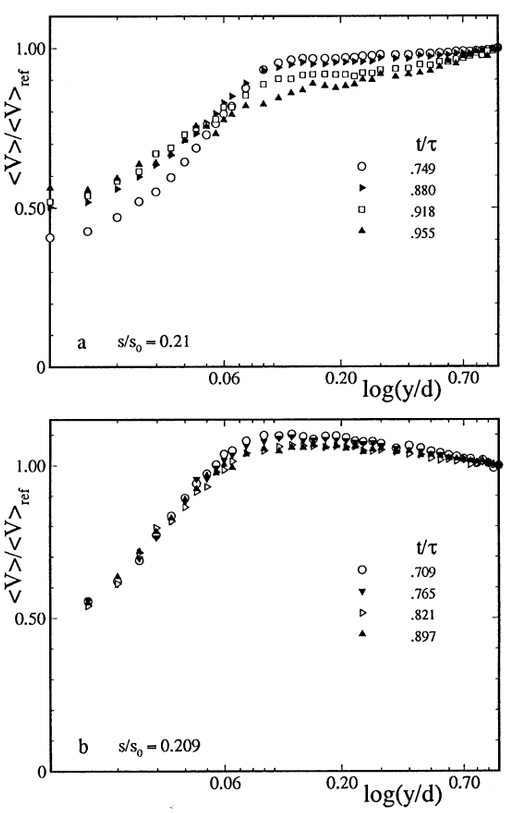

Fig. 5. Nondimensional velocity distribution on **a** pressure and **b** suction surfaces with time as parameter for $\Omega = 0.755$

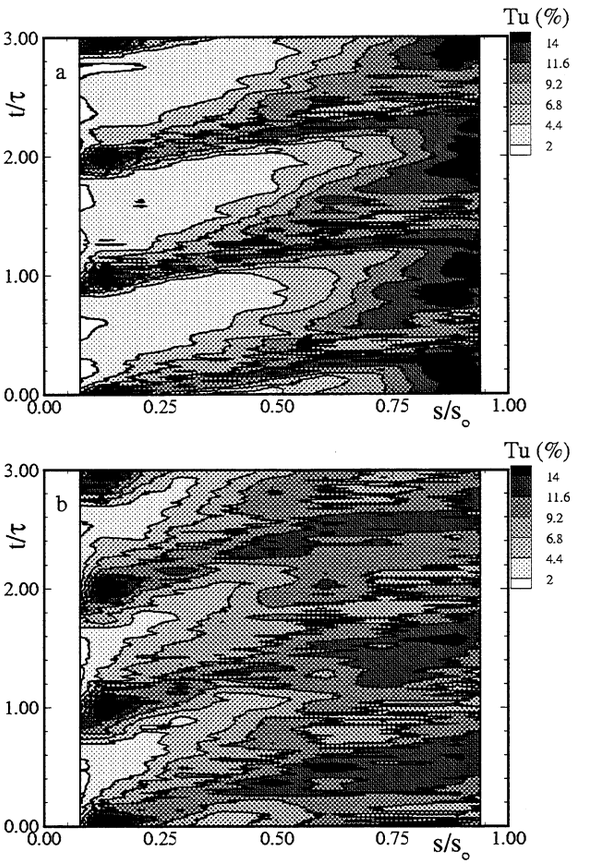

Fig. 6a, b. Ensemble-averaged turbulence intensity in temporal-spatial domain at $y = 0.5$ mm on pressure surface. **a** $\Omega = 0.755$; **b** $\Omega = 1.51$

The temporal-spatial distribution of the ensemble-averaged turbulence intensity for a lateral position of $y = 0.5$ mm on the pressure and suction surfaces for two different Ω-values is shown in Figs. 6 and 7. As shown in Fig. 6a, the boundary layer is periodically disturbed by the wakes that produce high turbulence intensity cores and extended becalmed regions ($Tu < 4.4\%$). The existence of a becalmed region was originally proposed by Schubauer and Klebanoff (1956) and investigated further in detail at Technical University of Darmstadt by Pfeil and his coworkers (Pfeil et al. 1983; Herbst 1980; Orth 1991). In a comprehensive study, Orth (1993) confirmed the propagation of leading and trailing edges of the wake strips at different velocities ($0.88U_\infty$, $0.5U_\infty$) and indicated that the faster moving turbulent strips inhibit the propagation of Tollmien–Schlichting waves at $0.29U_\infty$. Therefore, natural transition does not occur behind a turbulent strip, creating a becalmed region. The existence of becalmed regions in a curved plate boundary layer was discussed in detail by Schobeiri and Radke (1994b). The results presented in Figs. 6 and 7 generally confirm the findings by Orth (1993) and Schobeiri and Radke (1994b). On the pressure surface for $\Omega = 0.755$, the transition process starts at $s/s_0 = 0.5$, which is characterized by a steeper slope of turbulence intensity and

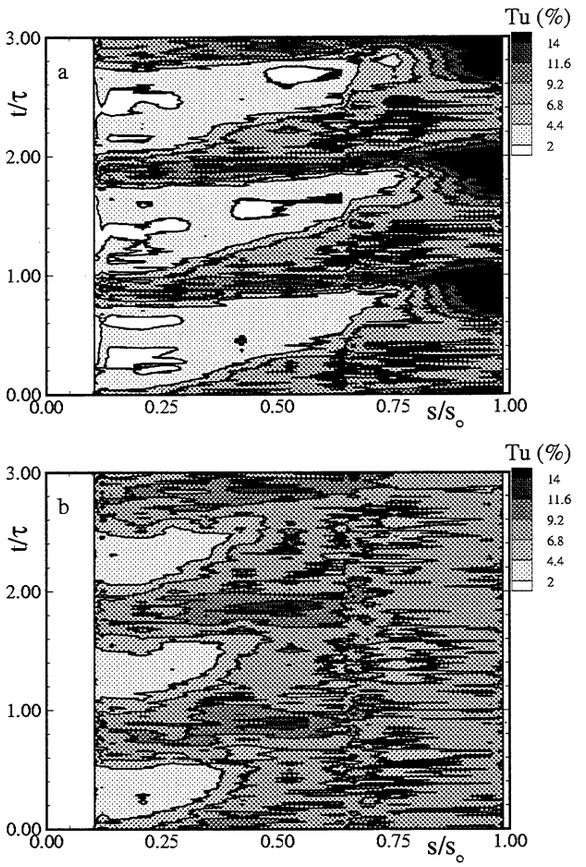

Fig. 7a, b. Ensemble-averaged turbulence intensity in temporal-spatial domain at $y=0.5$ mm on suction surface. **a** $\Omega=0.755$; **b** $\Omega=1.51$

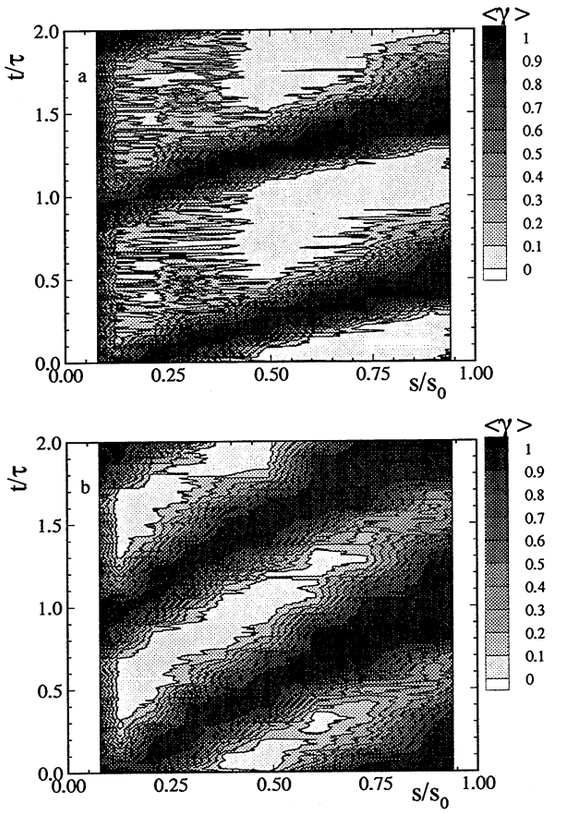

Fig. 8a, b. Ensemble-averaged intermittency factor distribution at $y=0.5$ mm on pressure surface. **a** $\Omega=0.755$; **b** $\Omega=1.51$

intermittency, Fig. 8a. Increasing Ω to 1.51, shown in Fig. 6b, causes an earlier mixing of impinging wakes that leads to narrower becalmed regions. The results on the suction surface, shown in Figs. 7a, b, can be similarly interpreted. A comparison of the pressure and suction surface turbulence intensity contour plots, Figs. 6a and 7a, indicates that the wake on the suction surface generates a higher turbulence intensity core starting at $s/s_0 \approx 0.25$, which coincides with the pressure minimum on the suction surface (Fig. 2). It is clear from Fig. 7a that the wake trailing edge, which is convecting downstream with lower velocity, does not have sufficient momentum to overcome the positive pressure gradient that prevails downstream of the pressure minimum. This leads to a stronger velocity deformation and thus stronger dissipation, which results in a narrower becalmed region compared to the pressure surface.

More detailed information about the complex transition process can be obtained from the ensemble-averaged intermittency $\langle\gamma\rangle$ contours shown in Figs. 8 and 9 for a lateral position of $y=0.5$ mm. The intermittency factor identifies the fraction of time during which the flow is turbulent. The details on the procedure to calculate the ensemble-averaged intermittency factor $\langle\gamma\rangle$ are available in a recent paper by Chakka and Schobeiri (1997). On the pressure surface, shown in Fig. 8a, the flow outside the wakes with a non-uniform intermittency distribution impinges on the blade surface. By convecting downstream, its turbulent fluctuations undergo a strong damping by the wall shear stress forces. The process of damping continues until $\langle\gamma\rangle$ reaches a minimum of 0.1 at $s/s_0 \approx 0.4$. This intermittency value is maintained over the remaining portion of the pressure surface indicating the intermittent character of the boundary layer. The intermittency distribution along the suction surface, Fig. 9a, reveals a substantially different character. Similar to Fig. 8a, it initially encounters a damping of the high intermittency flow outside the wakes. The damping process continues until $\langle\gamma\rangle$ reaches a minimum of 0.1 at $s/s_0 \approx 0.3$. At this point, the presence of a positive pressure gradient on the suction surface (Fig. 2) prevents any further damping, resulting in a small triangular becalmed region that extends up to $s/s_0 \approx 0.55$. By convecting downstream, an abrupt change in the direction of intermittency at a distance of $s/s_0=0.55$ is observed, which indicates the beginning of the boundary layer transition. We interpret this as representing a sudden shift from a flow dominated by the convection of wakes by the freestream to the propagation of boundary layer spots (or other turbulent structures) at a smaller speed. Increasing Ω to 1.51 on the pressure surface (Fig. 8b) causes an earlier mixing and stronger interaction of impinging wakes that leads to a narrower low-intermittency

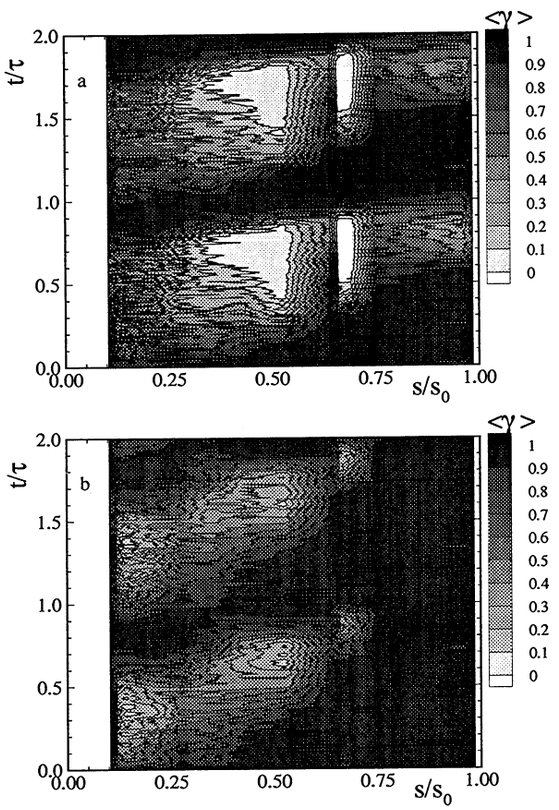

Fig. 9a, b. Ensemble-averaged intermittency factor distribution at $y = 0.5$ mm on suction surface. **a** $\Omega = 0.755$; **b** $\Omega = 1.51$

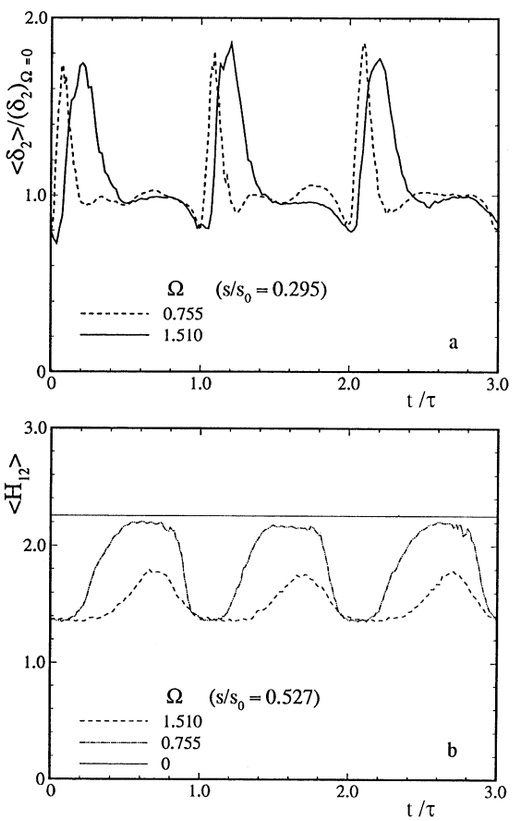

Fig. 10. Ensemble-averaged **a** momentum thickness on pressure surface and **b** shape factor on suction surface

region between the wakes. On the suction surface, (Fig. 9b), although the intermittency distribution shows similar tendencies as those discussed in reference to Fig. 9a, the values of the intermittency factor are relatively higher due to the higher Ω, which causes a strong interaction of wakes and an earlier mixing. For the case of $\Omega = 1.51$, the transition appears to have started around $s/s_0 \approx 0.5$ and is almost complete at $s/s_0 \approx 0.8$. While for $\Omega = 0.755$ (Fig. 9a), the transition starts around $s/s_0 \approx 0.55$ and is not yet complete at the trailing edge.

5.4
Boundary layer ensemble- and time-averaged integral quantities

The integral parameters, such as momentum thickness and shape factor, are of particular interest to a turbine designer, since they provide an accurate first estimation of the quality of the designed blade. The ensemble-averaged distributions of the momentum deficiency thickness and shape factor for the pressure and suction surfaces are shown in Fig. 10 for the two Ω values discussed earlier. The momentum thickness values are nondimensionalized with respect to the value corresponding to the steady case with $\Omega = 0$. The period τ represents to the wake-passing period that is specific to the individual wake generating cluster, which is characterized by the Ω-value under investigation. The periodic behavior of the ensemble-averaged momentum thickness on the pressure surface, at $s/s_0 = 0.295$, as a result of the embedded periodic wake flow, is clearly visible from Fig. 10a. It is also apparent from the figure that the effect of unsteadiness is to augment the momentum thickness. The shape factor $\langle H_{12} \rangle$ distribution on the suction surface at $s/s_0 = 0.527$ experiences a similar periodic change with an average below the steady case as shown in Fig. 10b. With increasing Ω-value, the time dependent distribution of the shape factor approaches a constant value that is far below the value measured for steady case. The implication is that unsteadiness hinders the tendency of separation. Other information regarding the overall evaluation of the turbine blade is provided by the time-averaged momentum thickness as shown in Fig. 11a, b for pressure and suction surfaces. The time-averaged momentum thickness indicates that for the *particular blade under investigation*, an increase of unsteady parameter Ω results in a consistent augmentation of the momentum thickness over the entire pressure and suction surfaces. Although a general conclusion cannot be drawn from these results, they show the impact of unsteady wake flow on the boundary layer parameters, and thus the profile loss coefficient and efficiency. This clearly shows that the steady state data cannot be transferred to the unsteady turbine design technology without modifications. It is necessary to emphasize the fact that the results, both qualitatively and quantitatively, represent the behavior pertaining to this particular low deflection blade under investigation. However, for a high

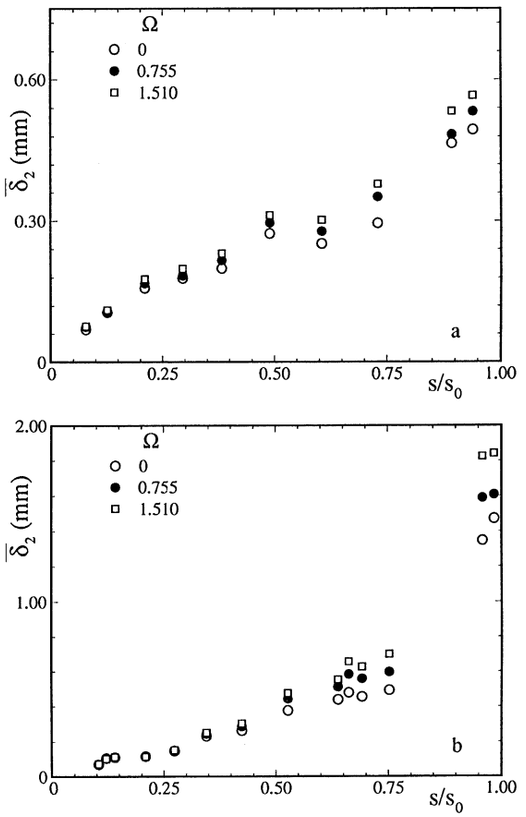

Fig. 11. Time-averaged momentum thickness on **a** pressure and **b** suction surfaces

deflection blade with a different pressure distribution, it is possible to have different values although they might still show similar qualitative behavior.

6 Conclusions

A detailed experimental study on the behavior of the unsteady boundary layer on a linear turbine cascade was presented. One steady and two different unsteady inlet wake flow conditions with the corresponding passing frequencies, wake structures, and freestream turbulence intensities were investigated utilizing a new large-scale, high-subsonic research facility. The two unsteady flow conditions were sequentially generated by two clusters of rods with the same diameter. The clusters were attached to two parallel timing belts with translational motion. The results of the comprehensive unsteady boundary layer measurements were presented in time-averaged, ensemble-averaged, and contour plot forms. The pressure distribution on the pressure side indicated a continuous acceleration of the flow, while on the suction side the initially strong acceleration was followed by a continuous mild deceleration that significantly influenced the unsteady boundary layer state. The unsteady wake flows characterized by the periodic asymmetric velocity distributions were clearly differentiable for small Ω-values. The time-averaged integral quantities indicated that for the *particular blade under investigation*, an increase of unsteady parameter Ω resulted in augmentation of the momentum deficiency thickness over the entire blade surface. The contour plots presented exhibit a clear picture of the unsteady boundary layer development indicating the effect of periodic wake flow, wake induced transition, and decay/mixing process that cause the final boundary layer transition.

References

Ashworth DA; LaGraff JE; Schultz DL; Grindrod KJ (1985) Unsteady aerodynamic and heat transfer processes in transonic turbine stage. ASME Paper 85-GT-128

Ashworth DA; LaGraff JE; Schultz DL (1989) Unsteady interaction effects on a turbine blade boundary layer. ASME J Turbomac 111: 162–168

Chakka P; Schobeiri MT (1997) Modeling unsteady boundary layer transition on a curved plate under periodic unsteady flow condition: aerodynamic and heat transfer investigations. In the review process

Doorly DJ; Oldfield MLG (1985a) Simulation of wake passing in a stationary turbine rotor cascade. J Propulsion 1: 316–318

Doorly DJ; Oldfield MLG (1985b) Simulation of the effects of shock wave on a turbine rotor blade. ASME Paper No. 85-GT-112

Dong Y; Cumpsty NA (1990a) Compressor blade boundary layers: Part 1 – test facility and measurement with no incident wakes. ASME J Turbomachinery 112: 231–240

Dong Y; Cumpsty NA (1990b) Compressor blade boundary layers: Part 2 – measurement with incident wakes. ASME J Turbomachinery 112: 222–230

Dring RP; Blair MF; Joslyn HD; Power GD; Verdon JM (1986) The effect of inlet turbulence and rotor/stator interactions on the aerodynamics and heat transfer of a large scale rotating turbine model. NASA CR 4079

Dullenkopf K; Schultz A; Wittig S (1991) The effect of incident wake conditions on the mean heat transfer of an airfoil. ASME J Turbomachinery 113: 412–418

Eifler I (1975) Zur Frage der freien turbulenten Strömungen, insbesondere hinter ruhenden und bewegten Zylindern. Dissertation D-17, Technische Hochschule Darmstadt, Germany

Herbst R (1980) Entwicklung von Strömungsgrenzsschichten bei instationärer Zuströmung in Turbomaschinen. Dissertation D-17, Technische Hochschule Darmstadt Germany

John J; Schobeiri T (1993) A simple and accurate method for calibrating X-Probes. J Fluid Eng, vol. 115, pp 148–152

Liu X; Rodi W (1989) Measurement of unsteady flow over and heat transfer from a flat plate. ASME Paper No. 89-GT-2

Liu X; Rodi W (1991) Experiments on transitional boundary layers with wake-induced unsteadiness. J Fluid Mech 231: 229–256

Mayle RE (1991) The role of Laminar-turbulent transition in gas turbine engines. ASME Paper No. 91-GT-261

Morehouse KA; Simoneau RJ (1986) Effect of a rotor wake on the local heat on the forward half of a circular cylinder. Proc 8th Int Heat Transfer Conf., San Francisco, California, pp 1249–1255

O'Brien JE; Simoneau RJ; LaGraff JE; Morehouse KA (1986) Unsteady heat transfer and direct comparison to steady state measurements in a rotor-wake experiment. Proc 8th Int Heat Transfer Conf., San Francisco, California, pp 1243–1248

O'Brien JE; Capp SP (1989) Two-component phase-averaged turbulent statistics downstream of a rotating spoked-wheel wake generator. ASME J Turbomachinery 111: 4 475–482

Orth U (1991) Entwicklung des instationären Nachlaufs hinter quer zur Strömungsrichtung bewegten Zylindern und dessen Einfluß auf das Umschlagverhalten von ebenen Grenzschichten stromabwärts angeordneter Versuchskörper. Dissertation D-17, Technische Hochschule Darmstadt

Orth U (1993) Unsteady boundary layer transition in flow periodically disturbed by wakes. ASME J Turbomachinery 115: 707–713

Pfeil H; Pache W (1977) Messungen von Strömungsgrenzschichten unter Turbo-maschinenbedingungen. Z Flugwiss Weltraumforsch 1: 267–278

Pfeil H; Herbst R (1979) Transition Procedure of Instationary Boundary Layers. ASME Paper No. 79-GT-128

Pfeil H; Herbst R; Schröder T (1983) Investigation of the laminar turbulent transition of boundary layers disturbed by wakes. ASME J Eng Power 105: 130–137

Poensgen C; Gallus HE (1991a) Three-dimensional wake decay inside of a compressor cascade and its influence on the downstream flow field: Part I – wake decay characteristics in the flow passage. ASME J Turbomachinery 113: 180–189

Poensgen C; Gallus HE (1991b) Three-dimensional wake decay inside a compressor cascade and its influence on the downstream flow field Part II – unsteady flow field downstream of the stator. ASME J Turbomachinery 113: 190–197

Priddy WJ; Bayley FJ (1988) Turbulence measurement in turbine blade passage and implications for heat transfer. ASME J Turbomachinery 110/73

Schobeiri MT; McFarland E; Yeh F (1991) Aerodynamics and heat transfer investigations on a high Reynolds number turbine cascade. NASA TM-103260

Schobeiri MT; John J (1994a) A study of the development of steady and periodic unsteady turbulent wakes through curved channels at positive, zero and negative pressure gradient. NASA Final Report, Part I, NAG 3-1256

Schobeiri MT; Radke RE (1994b) Effects of periodic unsteady wake flow and pressure gradient on boundary layer transition along the concave surface of a curved plate. Presented at the International Gas Turbine and Aeroengine Congress and Exposition, The Hague, Netherlands, 94-GT-327

Schobeiri MT; Pappu K; Wright L (1995) Experimental study of the unsteady boundary layer behavior on a turbine cascade. ASME Paper: 95-GT-435

Schubauer GB; Klebanoff PS (1956) Contributions on the mechanics of the boundary-layer transition. NACA Report, No. 1289

Schulte V; Hodson HP (1996) Unsteady wake-induced boundary layer transition in high lift LP turbines. ASME Paper No. 96-GT-486

Schultz HD; Gallus HE; Lakshminarayana B (1989) Three-dimensional separated flow field in the endwall region of an annular compressor cascade in presence of rotor-stator interaction, Part II: unsteady flow and pressure field. ASME Paper No. 89-GT-77

Simoneau RJ; Morehouse KA; Van Fossen GJ; Behnin FP (1984) Effect of a rotor wake on heat transfer from a circular cylinder. NASA TM 83613

Speidel L (1957) Beeinflussung der laminaren Grenzschicht durch periodische Störung der Zuströmung, Z Flugwiss Weetraumsforsch 5: 270–275

Trost N (1975) Einfluß der Zuströmturbulenz auf die Strömung in Axialgittern. Dissertation D-17, Technische Hochschule Darmstadt, Germany

Wittig S; Schultz A; Dullenkopf K; Fairbank J (1988) Effects of free-stream turbulence and wake characteristics on the heat transfer along a cooled gas turbine blade. ASME Paper No. 88-GT-179